

Electrical and thermal conductivity of liquid sodium from first-principles calculationsMonica Pozzo,¹ Michael P. Desjarlais,² and Dario Alfè^{1,*}¹*Department of Earth Sciences, Department of Physics and Astronomy, London Centre for Nanotechnology and TYC@UCL, University College London, Gower Street, London WC1E 6BT, United Kingdom*²*Pulsed Power Sciences Center, Sandia National Laboratories, Albuquerque, New Mexico 87185, USA*

(Received 23 May 2011; published 4 August 2011)

We report on the electrical and thermal conductivity of liquid sodium at 400 K, calculated using density functional theory with the local density approximation (LDA) and the Kubo-Greenwood formula. We extensively tested system-size errors and \mathbf{k} -point sampling, using simulation cells containing up to 2000 atoms. We find that convergence of the results with respect to the size of the system is slow, and at least 1024-atom systems are required to obtain conductivities converged to within a few percent. Γ -point sampling does not seem to be accurate enough, even for the very largest 2000-atom system. We performed calculations at three densities, including the experimental density $\rho_{\text{expt}} = 921 \text{ kg m}^{-3}$, the LDA density $\rho_{\text{LDA}} = 1046 \text{ kg m}^{-3}$, and a higher density $\rho = 1094 \text{ kg m}^{-3}$. At the experimental density, the electrical conductivity is underestimated by $\sim 35\%$, at the LDA density it is overestimated by $\sim 18\%$, and at the largest density it is higher than the experimental one by $\sim 50\%$. At the experimental density, we also used the Perdew-Burke-Ernzerhof functional, and found that the conductivity is overestimated by only $\sim 6\%$.

DOI: [10.1103/PhysRevB.84.054203](https://doi.org/10.1103/PhysRevB.84.054203)

PACS number(s): 72.15.Cz, 71.15.-m, 65.20.-w

I. INTRODUCTION

Because of its simplicity and resemblance to an ideal free-electron system, sodium is one of the most studied metals. Liquid sodium is particularly interesting from a scientific and technological point of view. For example, it is used as coolant in fast-breeding nuclear reactors, and in heat pipes in high-temperature solar-energy power plants, thanks to its large thermal conductivity, which makes it a very effective heat-transfer medium. It also has useful properties such as low vapor pressure and high boiling point, low viscosity and density, and being a low neutron absorber.¹ Recently, liquid sodium was used as a proxy to study the self-sustained geomagnetic field, generated in the liquid part of the Earth's core. Despite the experiments being obviously performed on much different size and time scales, the parameters were tuned to reproduce the relevant conditions representative of the Earth's core.² Among the various parameters entering the magnetohydrodynamics equations used to describe the self-generation of a magnetic field in a rotating liquid metal, particularly important ones are the electrical and the thermal conductivity of the metal.

The electrical conductivity of liquid sodium has been calculated by several groups in the past,³⁻⁶ mainly using the phenomenological approach of Ziman⁷ based on the structure factor of the liquid. More recently, a direct approach based on the Kubo-Greenwood (KG) formula^{8,9} in combination with density functional theory (DFT) was employed by Silvestrelli *et al.*¹⁰ and by Knider *et al.*¹¹ In principle, the KG formula is exact, but the use of the DFT single-particle orbitals (in addition to inaccuracies of the exchange-correlation functional) makes its application imperfect. Silvestrelli *et al.*¹⁰ found that the calculated conductivity of Na near the melting point is underestimated by DFT with the local density approximation (LDA) roughly by a factor of 2, although the agreement between calculations and experiments improves as the temperature is raised. They argued that this disagreement is probably due to the use of DFT-LDA orbitals in the KG

formula, and to the size of their simulation cells, which included up to 206 atoms. By contrast, Knider *et al.*¹¹ obtained a value for the electrical conductivity of liquid Na near its melting point very close to the experimental one, even though they used much smaller simulation cells including only 32 atoms. Both Silvestrelli *et al.*¹⁰ and Knider *et al.*¹¹ performed the calculations at the experimental density.

Here, we have revisited the problem and investigated the electrical conductivity of liquid sodium at 400 K using DFT-LDA and the KG formula. Thanks to big advancements in computer power in recent years, we have been able to investigate size effects using simulation cells containing up to 2000 atoms. In order to investigate the effect of density on the conductivity, we performed calculations at the experimental density $\rho_{\text{exp}} = 921 \text{ kg m}^{-3}$,¹² the LDA density $\rho_{\text{LDA}} = 1046 \text{ kg m}^{-3}$,¹³ and the density $\rho = 1094 \text{ kg m}^{-3}$. Our results at the experimental density lead to similar conclusions as those of Silvestrelli *et al.*¹⁰ in that they underestimate the electrical conductivity, even though by only 35%, and shed new light on the magnitude of size effects. In particular, we found that these errors are significant on systems including less than ~ 1000 atoms. At the LDA density, the conductivity is overestimated by $\sim 18\%$, and at the higher density, we found that the conductivity is higher than the experimental one by $\sim 50\%$.

We also investigated the effect of using the Perdew-Burke-Ernzerhof¹⁶ (PBE) functional and found that, at the experimental density, the results are in much better agreement with experiments, overestimating the conductivity by only $\sim 6\%$.

As a by-product of our simulations, we obtained the electronic component of the thermal conductivity, which shows that, as expected for an almost free-electron-like system such as liquid Na, the Wiedemann-Franz law¹⁷ is closely obeyed, with a Lorenz number close to the ideal value $\sim 2.44 \times 10^{-8} \text{ } \Omega \text{ W K}^{-2}$ at all densities.

The paper is organized as follows. In the next section, we describe the techniques and the computational framework. In

Sec. III, we present the results, beginning with the structural properties of liquid Na, followed by a report on the electrical and thermal conductivity. Section IV contains our conclusions.

II. TECHNIQUES

First-principles simulations were performed using the VASP code¹⁸ with the projector augmented wave (PAW) method^{19,20} and the LDA or the PBE (Ref. 16) functional. Most calculations were performed with a Na PAW with only the $3s$ electron in valence, but we also tested the effect of including the $2p$ electrons in valence, which showed an undetectable effect on the conductivities. Single-particle orbitals were expanded in plane waves with a cutoff of 102 and 300 eV for the PAWs with the $3s^1$ and $2p^63s^1$ valence configurations, respectively, and the core radii were 1.16 Å in both cases. Electronic levels were occupied according to Fermi-Dirac statistics, with an electronic temperature of 0.035 eV. An efficient extrapolation of the charge density was used to speed up the *ab initio* molecular dynamics calculations.²¹ The simulations were performed by sampling the Brillouin zone (BZ) with the Γ point only. The temperature was controlled with a Nosé thermostat²² and the time step was set to 3 fs. We used simple cubic simulation cells including 54, 128, 432, 1024, 1458, and 2000 atoms. For each size, we started from a perfect body-centred-cubic (bcc) lattice and melted the system by simulating for 3 ps at a temperature of 4000 K. We monitored the system by calculating the time-dependent mean-square displacement and verified that, after 3 ps, a good equilibrated liquid was obtained. After that, we reduced the temperature to 400 K and rethermalized the system for further 3 ps. Then, we simulated for an additional 15 ps from which we extracted $N = 10$ configurations $\{R_I; I = 1, N\}$ equally spaced in time. These N configurations were then used to compute the electrical and the thermal conductivity via the Kubo-Greenwood and the Chester-Thellung-Kubo-Greenwood²³ formula, respectively, as implemented in VASP.²⁴

The Kubo-Greenwood formula for the electrical conductivity as a function of frequency ω for a particular \mathbf{k} point in the BZ of the simulation supercell and for a particular configuration of the ions $\{R_I\}$ reads as

$$\sigma_{\mathbf{k}}(\omega; R_I) = \frac{2\pi e^2 \hbar^2}{3m^2 \omega \Omega} \sum_{i,j=1}^n \sum_{\alpha=1}^3 [F(\epsilon_{i,\mathbf{k}}) - F(\epsilon_{j,\mathbf{k}})] \times |(\Psi_{j,\mathbf{k}} | \nabla_{\alpha} | \Psi_{i,\mathbf{k}})|^2 \delta(\epsilon_{j,\mathbf{k}} - \epsilon_{i,\mathbf{k}} - \hbar\omega), \quad (1)$$

where e and m are the electron charge and mass, respectively, \hbar is the Planck's constant divided by 2π , Ω is the volume of the simulation cell, and n is the number of Kohn-Sham states. The α sum runs over the three spatial directions, which in a liquid are all equivalent. $\Psi_{i,\mathbf{k}}$ is the Kohn-Sham wave function corresponding to eigenvalue $\epsilon_{i,\mathbf{k}}$, and $F(\epsilon_{i,\mathbf{k}})$ is the Fermi weight. The δ function is represented by a Gaussian, with a width chosen to be roughly equal to the average spacing between the eigenvalues weighted by the corresponding change in the Fermi function.²⁴ The width was chosen to be 45, 18, 5, 2.2, 1.7, and 1.2 meV for the 54-, 128-, 432-, 1024-, 1458-, and 2000-atom systems,

respectively. Integration over the BZ is performed using standard methods,²⁵ and the frequency-dependent conductivity of the liquid is obtained by averaging over the N configurations $\{R_I; I = 1, N\}$:

$$\sigma(\omega) = \frac{1}{N} \sum_{I=1}^N \sum_{\mathbf{k}} \sigma_{\mathbf{k}}(\omega; R_I) W(\mathbf{k}). \quad (2)$$

Here, $W(\mathbf{k})$ is the weighting factor for the point \mathbf{k} . In principle, all the $W(\mathbf{k})$ would be identical for a simulation with no symmetries like that of a liquid in a cubic box. In practice, we found it convenient to use \mathbf{k} points drawn from the irreducible wedge of the BZ of the same system in which the atoms occupy bcc perfect lattice positions, as convergence with respect to the number of \mathbf{k} points is faster if the points are chosen in this way [in the case of one \mathbf{k} point only, this corresponds to the Baldereschi point,²⁶ given by $(2\pi/a)(1/4, 1/4, 1/4)$, where a is the length of the side of the cubic simulation box]. The dc conductivity σ_0 is given by the value of $\sigma(\omega)$ in the limit $\omega \rightarrow 0$. This limit needs to be taken with care because, at very small values of ω , the conductivity falls unphysically to zero due to the artificial finite spacing between the Kohn-Sham eigenvalues, caused by the finite size of the simulation cell. To take this limit, our procedure is to fit the conductivity to a smooth function, without including in the fit values of $\sigma(\omega)$ that have started to fall to zero. Since liquid Na is a nearly free-electron metal, the optical conductivity is expected to behave according to a Drude model $\sigma(\omega) = \sigma_0/(1 + \omega^2\tau^2)$, with τ being the relaxation time, which is what we chose to fit the data.

The optical conductivity must obey the sum rule

$$S = \frac{2m\Omega}{\pi e^2 N_e} \int_0^{\infty} \sigma(\omega) d\omega = 1, \quad (3)$$

where N_e is the number of electrons in the simulation cell. The value of S provides a useful check of the quality of the data, although in practice it is expected to be less than one, as only states up to a finite value of ω can be included in the calculations. However, the low-energy part of $\sigma(\omega)$, which is used to extract the dc conductivity, converges much faster than the high-energy tail. We decided to include in the calculations only states up to 2 eV above the Fermi energy, and verified that the low-energy part of the spectrum is unaffected by this choice by performing spot checks in which we included states up to 5 eV above the Fermi energy.

In a free-electron liquid, the electronic part of the thermal conductivity κ_0 and the electrical conductivity σ_0 are related by the Wiedmann-Franz law $L = \kappa_0/\sigma_0 T$, where L is the Lorenz number. Here, we have directly calculated κ_0 using the Chester-Thellung²³ formulation of the Kubo-Greenwood formula, which reads as

$$\kappa(\omega) = \frac{1}{e^2 T} \left(L_{22}(\omega) - \frac{L_{12}(\omega)^2}{\sigma(\omega)} \right), \quad (4)$$

and κ_0 is the value of $\kappa(\omega)$ in the limit $\omega \rightarrow 0$. The kinetic

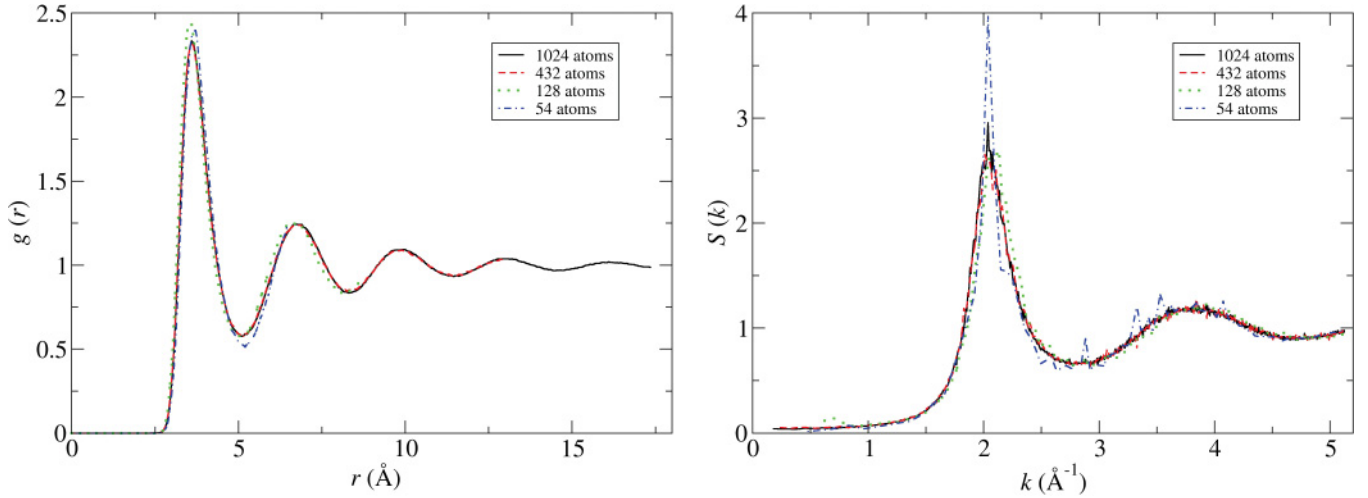


FIG. 1. (Color online) Radial distribution function $g(r)$ (left panel) and structure factor $S(k)$ (right panel) of liquid Na at 400 K at the experimental density $\rho_{\text{expt}} = 921 \text{ kg m}^{-3}$, computed using simulation cells including 54, 128, 432, and 1024 atoms. Data from simulations with 1458 and 2000 atoms are indistinguishable from those with 1024 atoms and are not shown. All simulations have been performed with the Γ point only.

coefficients $L_{lm}(\omega)$ are given by²⁷

$$L_{lm}(\omega) = (-1)^{(l+m)} \frac{2\pi e^2 \hbar^2}{3m^2 \omega \Omega} \sum_{i,j=1}^n \sum_{\alpha=1}^3 [F(\epsilon_{i,\mathbf{k}}) - F(\epsilon_{j,\mathbf{k}})] \\ \times |\langle \Psi_{j,\mathbf{k}} | \nabla_{\alpha} | \Psi_{i,\mathbf{k}} \rangle|^2 [\epsilon_{j,\mathbf{k}} - \mu]^{(l-1)} [\epsilon_{i,\mathbf{k}} - \mu]^{(m-1)} \\ \times \delta(\epsilon_{j,\mathbf{k}} - \epsilon_{i,\mathbf{k}} - \hbar\omega), \quad (5)$$

where μ is the chemical potential.

III. RESULTS

In Fig. 1 (left panel), we show the radial distribution functions $g(r)$ of liquid Na at 400 K computed with simulation cells containing 54, 128, 432, and 1024 atoms. The simulations

were performed using the Γ point only at the experimental density $\rho_{\text{expt}} = 921 \text{ kg m}^{-3}$. Size effects are apparent for the 54- and the 128-atom systems, but for sizes including 432 atoms or more, the calculated $g(r)$ are indistinguishable from each other. The same size effects can be observed in the structure factor $S(k)$ (Fig. 1, right panel). The $g(r)$ and $S(k)$ for the 1458- and 2000-atom systems are also essentially identical to those of the 432- and 1024-atom systems, and are not shown.

In Fig. 2, we plot the radial distribution function $g(r)$ both at the experimental density $\rho_{\text{expt}} = 921 \text{ kg m}^{-3}$ and at the LDA density $\rho_{\text{LDA}} = 1046 \text{ kg m}^{-3}$. We also plot the structure factor calculated at the two densities, and we compare it with experimental data, taken at 373 K.²⁸ We see that the $S(k)$ calculated at the experimental density agrees well with the experimental structure factor, and the agreement is less good when the LDA density is used in the calculations. The present

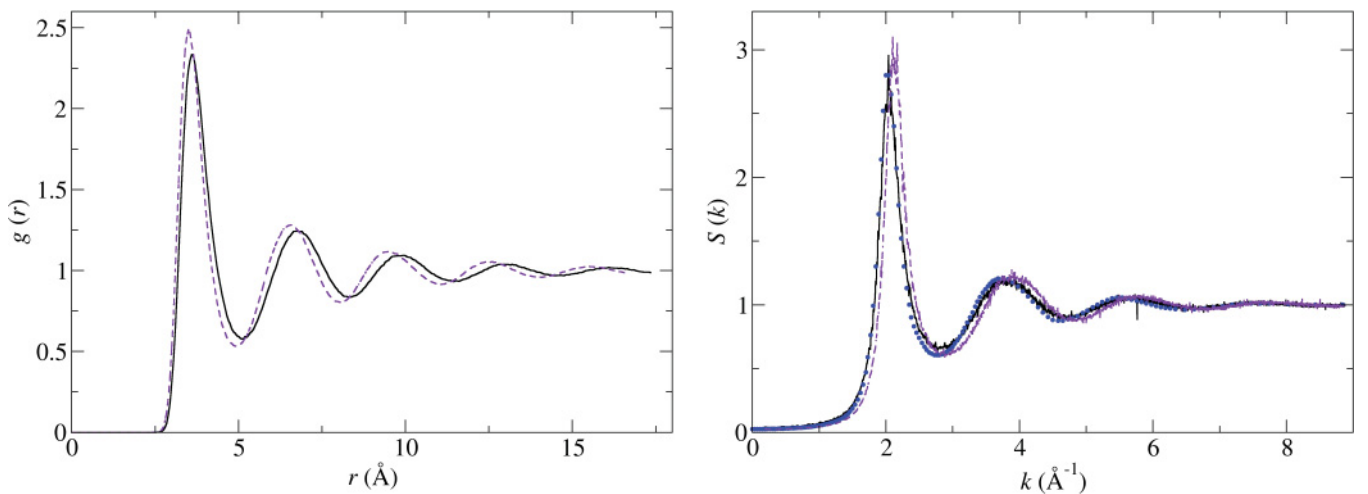


FIG. 2. (Color online) Radial distribution function $g(r)$ (left panel) and structure factor $S(k)$ (right panel) of liquid Na at 400 K, computed using 1024-atom simulation cells at the experimental density $\rho_{\text{expt}} = 921 \text{ kg m}^{-3}$ (black solid curve) and at the LDA density $\rho_{\text{LDA}} = 1046 \text{ kg m}^{-3}$ (dashed violet curve). Experimental data (blue dots) are from Ref. 28.

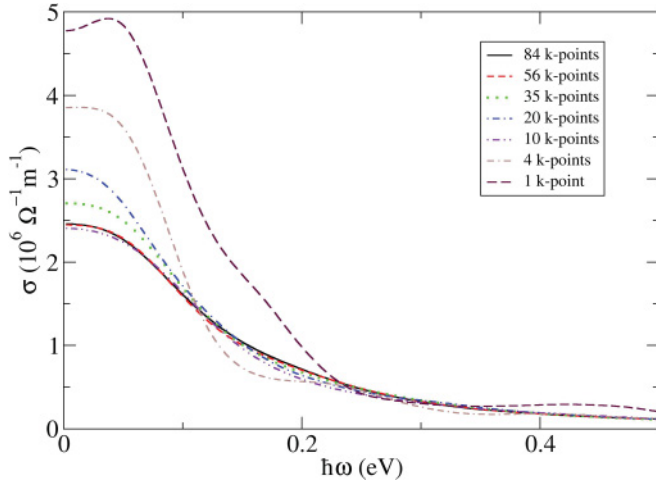


FIG. 3. (Color online) Optical conductivity $\sigma(\omega)$ at the experimental density, calculated with the 54-atom system and using various sets of \mathbf{k} points.

results are in good agreement with previous DFT studies of liquid Na.^{10,11,29}

In Fig. 3, we show the optical conductivity for the smaller 54-atom system, calculated as described in Sec. II and as function of number of \mathbf{k} points. The data show that $\sigma(\omega)$ strongly depends on the number of \mathbf{k} points included in the calculations and demonstrate that, for this system size, one needs to include at least 56 \mathbf{k} points for the results to be completely converged.

In Fig. 4, we show the conductivity as function of system size, calculated with the Γ point only. The smallest 54-atom system is not included because Γ -only sampling induces an artificial gap of ~ 0.5 eV, which is large enough to produce an unphysical very small conductivity. It is clear that convergence with respect to system size is very slow, and the results still show differences between the two largest 1458- and 2000-atom systems. Even with the 2000-atom systems, the results are not converged yet (see below). This confirms previous suggestions¹⁰ that Γ -point-only sampling is not sufficient, but

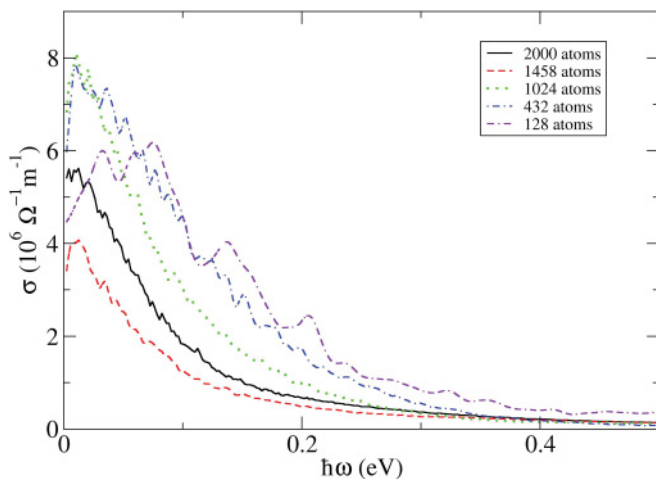


FIG. 4. (Color online) Optical conductivity $\sigma(\omega)$ at the experimental density calculated with the Γ point only for various system sizes.

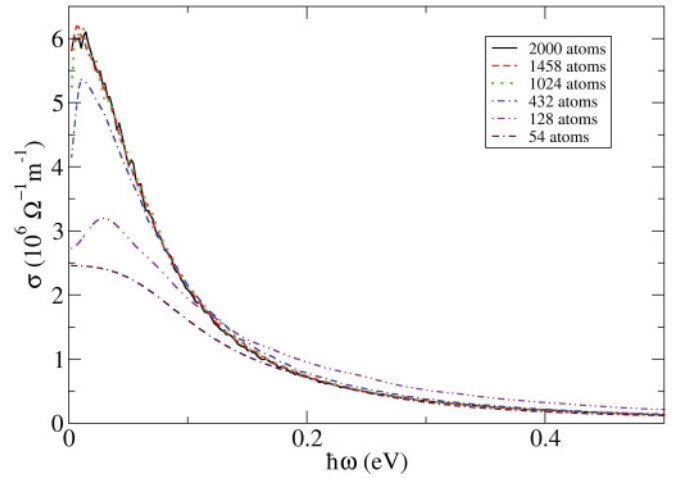


FIG. 5. (Color online) Optical conductivity $\sigma(\omega)$ at the experimental density calculated with the 54-, 128-, 432-, 1024-, 1458-, and 2000-atom systems. Results shown are fully converged with respect to \mathbf{k} -point sampling.

extends the claim to much larger systems than previously explored.

Convergence of the results with respect to \mathbf{k} points is expected to be faster for larger systems, and this is indeed what we observe. For instance, in order to obtain conductivities converged to within 1%, we need 10 \mathbf{k} points for the 128-atom system, 4 for the 432-atom system, and just the Baldereschi point²⁶ for the systems with 1024 atoms and above. In Fig. 5, we show the optical conductivity for various system sizes, where only the \mathbf{k} -point converged result for each size is shown. At variance with the previous Γ -point case, we observe that convergence with respect to system size is indeed obtained. However, even with a 432-atom system, the error in the optical conductivity is still appreciable.

The dc conductivities have been obtained by fitting the low-energy region of the optical conductivity to a Drude function, which as expected adapts to the data very well. The results are summarized in Fig. 6. The first thing to notice is that, as mentioned above, Γ -point sampling is inadequate even for the largest systems. On the other hand, the Baldereschi point²⁶ provides good results, as long as at least 1024 atoms are included in the simulation cell. In fact, it is clear that, even with 432-atom cells, the error in the conductivity is at least $\sim 10\%$. We also display in Fig. 6 the value of S , which shows that the sum rule is closely satisfied, a part from the simulations with the Γ point and those with the small 54-atom system.

Our results come to the same conclusions as those of Silvestrelli *et al.*,¹⁰ namely, that, at the experimental density, the dc conductivity predicted by LDA is lower than the experimental one. The use of larger simulation cells improves the results to the value $\sigma_0 = 6.2 \times 10^6 \Omega^{-1} \text{m}^{-1}$, but this is still $\sim 35\%$ lower than the experimental value $\sigma_0^{\text{expt}} = 9.7 \times 10^6 \Omega^{-1} \text{m}^{-1}$.³⁰

To investigate the dependence of the conductivity on the density of the system, we performed calculations also at LDA density $\rho_{\text{LDA}} = 1046 \text{ kg m}^{-3}$ and at the density $\rho = 1094 \text{ kg m}^{-3}$. At the highest density, we repeated all the size and \mathbf{k} -points tests performed for the system at the

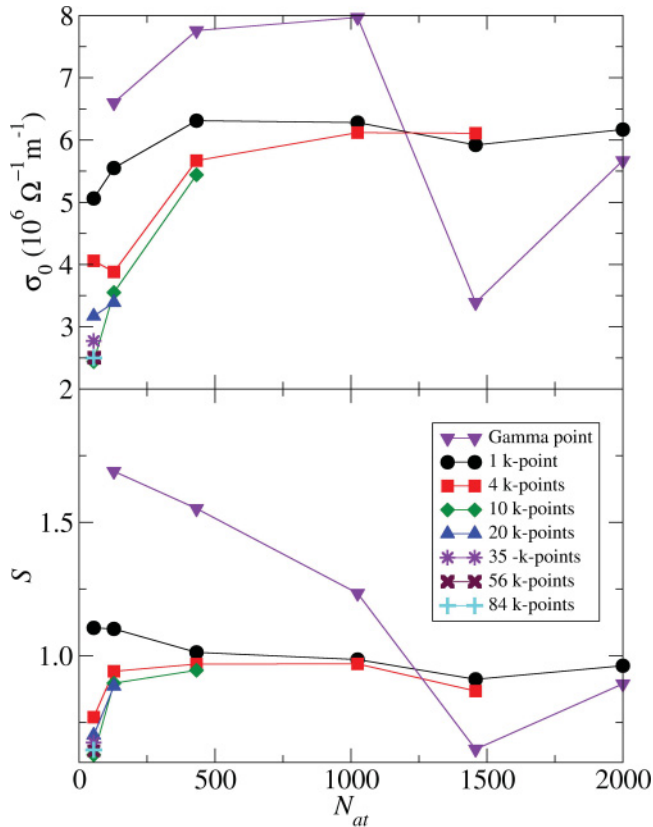


FIG. 6. (Color online) Electrical conductivity σ_0 (top panel) obtained from a fit of $\sigma(\omega)$ to a Drude function for the 54-, 128-, 432-, 1024-, 1458-, and 2000-atom systems at the experimental density $\rho_{\text{expt}} = 921 \text{ kg m}^{-3}$. Bottom panel shows the value of S [see Eq. (3)]. Results are shown for various sets of \mathbf{k} points.

experimental density, and the results are summarized in Fig. 7. At the LDA density, we only performed the calculations on the 1024-atom system. We found that the dc conductivities are $\sigma_0 = 11.4 \times 10^6 \Omega^{-1} \text{ m}^{-1}$ and $\sigma_0 = 14.6 \times 10^6 \Omega^{-1} \text{ m}^{-1}$ in the two cases, respectively, which are $\sim 18\%$ and $\sim 50\%$ higher than the experimental one, respectively. The much closer agreement between the calculations performed at the LDA density and the experimental data is encouraging, and supports the *first-principles* approach in which no experimental input is provided to the calculations. On this point, we should also note that the conductivity depends significantly on temperature, or rather on the distance from the melting temperature, so it is possible that the remainder of the disagreement with the experimental data is due to that. At present, the zero-pressure LDA melting temperature of Na is not yet known.

Finally, to test the effect of Brillouin zone sampling on the geometry of the system and how this could possibly propagate to the conductivity, we performed a further simulation with the 1024-atom system at the experimental density using the Baldereschi point.²⁶ From this simulation, we obtained a radial distribution function, which is indistinguishable from that obtained with the Γ -point simulation, and the calculated electrical conductivity is also essentially identical in the two cases.

It is interesting to investigate the effect of the exchange-correlation functional on the conductivity of Na. For this reason, we performed an additional simulation

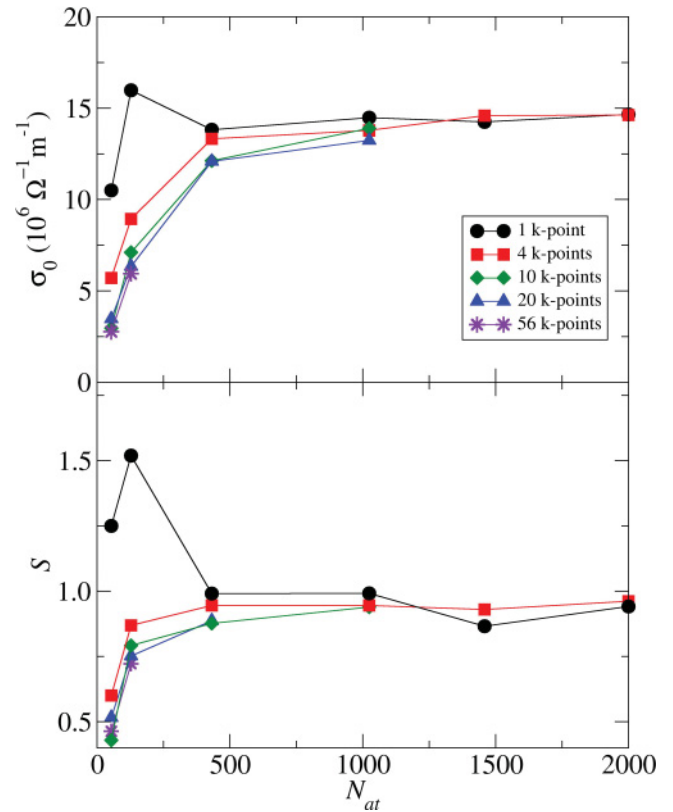


FIG. 7. (Color online) Electrical conductivity σ_0 (top panel) obtained from a fit of $\sigma(\omega)$ to a Drude function for the 54-, 128-, 432-, 1024-, 1458-, and 2000-atom systems at the density $\rho = 1094 \text{ kg m}^{-3}$. Bottom panel shows the value of S [see Eq. (3)]. Results are shown for various sets of \mathbf{k} points.

on the 1024-atom system using the PBE functional at the experimental density $\rho_{\text{expt}} = 921 \text{ kg m}^{-3}$, which is very close to the PBE density $\rho_{\text{PBE}} = 926 \text{ kg m}^{-3}$.¹³ As in the previously described cases, we extracted 10 statistically independent configurations to compute the conductivity, and obtained the value $\sigma_0 = 10.3 \times 10^6 \Omega^{-1} \text{ m}^{-1}$, which is only $\sim 6\%$ higher than the experimental value.

The calculation of the electronic component of the thermal conductivity κ was performed using Eqs. (4) and (5), and it was computed simultaneously to the electrical conductivity σ . The size and \mathbf{k} -point effects discussed for the computation of $\sigma(\omega)$ also apply to the calculation of $\kappa(\omega)$. By extrapolating $\kappa(\omega)$ for $\omega \rightarrow 0$, we obtain the value of $\kappa_0 = 60 \text{ W m}^{-1} \text{ K}^{-1}$ when we use the experimental density, $\kappa_0 = 107 \text{ W m}^{-1} \text{ K}^{-1}$ at the LDA density, and $\kappa_0 = 140 \text{ W m}^{-1} \text{ K}^{-1}$ when we use the density $\rho = 1094 \text{ kg m}^{-3}$. When compared to the experimental value $\kappa_0^{\text{expt}} = 86 \text{ W m}^{-1} \text{ K}^{-1}$,³¹ these values display a similar degree of accuracy as the electrical conductivity. Using the PBE functional and the experimental density, we obtained $\kappa_0 = 93 \text{ W m}^{-1} \text{ K}^{-1}$. The Lorenz numbers are $L = 2.42, 2.34, 2.4$, and $2.26 \times 10^{-8} \Omega \text{ W K}^{-2}$ for the three LDA cases and the PBE case, respectively, very close to the ideal value. The electrical and thermal conductivity results are summarized in Table I.

To understand in more details why convergence with respect to the size of the system is so difficult, we plot in Fig. 8 the density of the represented states and the derivative of the Fermi

TABLE I. Electrical dc conductivity σ_0 , thermal conductivity κ_0 , and Lorenz number L of liquid sodium calculated in this paper at various densities and $T = 400$ K, compared with experimental data at ambient pressure (in square brackets). Calculations have been performed using the LDA and PBE (values in parentheses).

ρ (kg m ⁻³)	σ_0 (10 ⁶ Ω^{-1} m ⁻¹)	κ_0 (W m ⁻¹ K ⁻¹)	L (10 ⁻⁸ Ω W K ⁻²)
[921] ^a	6.2 (10.3) [9.7] ^b	60 (93) [86] ^c	2.42(2.26)[2.22] ^c
1046	11.4	107	2.34
1094	14.6	140	2.4

^aReference 12.

^bReference 30.

^cReference 31.

distribution with respect to the energy $dF/d\epsilon$ divided by its value at the minimum (i.e., at the Fermi energy). The plot is restricted to the region where $dF/d\epsilon$ is appreciably different from zero, which is the only region contributing to the dc conductivity. The left panel of the figure is for the 128-atom system, and the right panel is for the 1024-atom system. It is clear that, for the small system, there are only a few states that contribute to the conductivity, and for this reason the calculations with a system of this size are not accurate enough.

IV. CONCLUSIONS

We have presented first-principles calculations of the electrical and thermal conductivity of liquid Na at a temperature of 400 K. The calculations are based on density functional theory with the local density approximation and the Kubo-Greenwood formula. We have shown that size effects are not trivial in this system, and unexpectedly large simulation cells are required to converge the results to high accuracy. We have also shown that \mathbf{k} -point sampling is crucial, and even with a very large system containing 2000 atoms, using only the Γ point gives results that are simply not converged. The possibility of large size effects had been already mentioned in previous work,¹⁰ but here we have explicitly addressed their magnitudes.

The calculated value of the electrical conductivity at the experimental density is too low by $\sim 35\%$, in general agreement with previous calculations. We have also investigated the effect of the density on the conductivity, and we found that the LDA

performs better at the LDA density. Moreover, the conductivity depends strongly on temperature, and presumably on how far the system is from the melting temperature. This would suggest that it should be interesting to compute the zero-pressure LDA melting point of Na, and investigate the dependence of the calculated values of the conductivities as a function of distance from the calculated melting temperature. As pointed out earlier,¹⁰ an additional source of error could be the use of the DFT eigenvalues and eigenstates in the Kubo-Greenwood formula instead of the true many-body values. This error is not confined to the use of the LDA, as even if we knew the exact exchange-correlation functional, the single-particle eigenvalues and eigenstates would still not be the correct quantities to use.

Finally, we tested the effect of using the PBE exchange-correlation functional instead of the LDA and found that the PBE functional gives better agreement with the experimental density. Likewise, PBE gives significantly better agreement with the measured conductivity, and at the experimental density, the calculated conductivity is only $\sim 6\%$ too high. Given the observed high sensitivity of the conductivity on the density, this could be the reason why the PBE is much more accurate.

The electronic part of the thermal conductivity is computed using essentially the same ingredients as those employed for the electrical conductivity, and the results show that the Wiedemann-Franz law is closely satisfied, as expected for a nearly free-electron metal such as sodium.

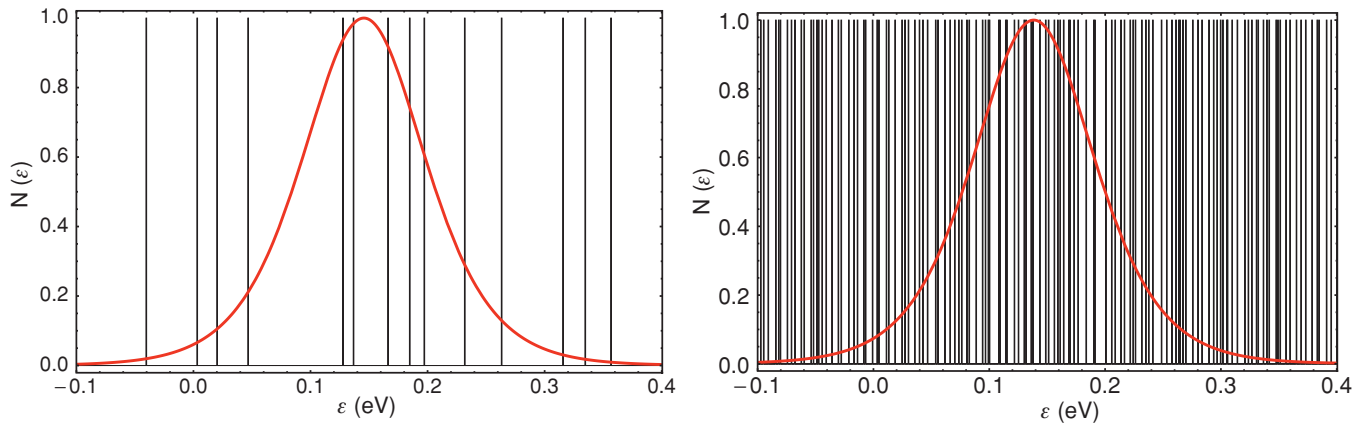


FIG. 8. (Color online) Density of represented states $N(\epsilon)$ (vertical black lines) and derivative of the Fermi distribution $dF/d\epsilon$ divided by its value at the minimum (red curve) for the 128-atom (left panel) and the 1024-atom (right panel) systems. Apparent thicker lines correspond to nearly degenerate eigenvalues.

ACKNOWLEDGMENTS

The work of M.P. and D.A. was conducted as part of a EURYI scheme award as provided by EPSRC

(see www.esf.org/euryi). Calculations were performed on the HECToR service in the UK We thank two anonymous referees for valuable suggestions.

*d.alf@ucl.ac.uk

- ¹R. D. Kale and M. Rajan, *Curr. Sci. India* **86**, 668 (2004).
- ²P. Cardin, D. Brito, D. Jault, H.-C. Nataf, and J.-P. Masson, *Magnetohydrodynamics (NY)* **38**, 177 (2002).
- ³M. P. Greene and W. Kohn, *Phys. Rev.* **137**, A513 (1965).
- ⁴N. W. Ashcroft and J. Lekner, *Phys. Rev.* **145**, 83 (1966).
- ⁵J. F. Devlin and W. van der Lugt, *Phys. Rev. B* **6**, 4462 (1972).
- ⁶S. Sinha, P. L. Srivastava, and R. N. Singh, *J. Phys. Condens. Matter* **1**, 1695 (1989).
- ⁷J. M. Ziman, *Philos. Mag.* **6**, 1013 (1961).
- ⁸R. Kubo, *J. Phys. Soc. Jpn.* **12**, 570 (1957).
- ⁹D. A. Greenwood, *Proc. Phys. Soc., London* **71**, 585 (1958).
- ¹⁰P. L. Silvestrelli, A. Alavi, and M. Parrinello, *Phys. Rev. B* **55**, 15515 (1997).
- ¹¹F. Knider, J. Hugel, and A. V. Postnikov, *J. Phys. Condens. Matter* **19**, 196105 (2007).
- ¹²P. Yu. Os'minin, *J. Eng. Phys. Thermophys.* **8**, 334 (1965).
- ¹³This was obtained by simulating the liquid at constant zero pressure, with an algorithm (Ref. 14) recently implemented in VASP (Ref. 15).
- ¹⁴E. R. Hernández, *J. Chem. Phys.* **115**, 10282 (2001).
- ¹⁵E. R. Hernández, A. Rodríguez-Prieto, A. Bergara, and D. Alfè, *Phys. Rev. Lett.* **104**, 185701 (2010).
- ¹⁶J. P. Perdew, K. Burke, and M. Ernzerhof, *Phys. Rev. Lett.* **77**, 3865 (1996).
- ¹⁷D. Wiedemann and R. Franz, *Ann. Phys. (NY)* **165**, 497 (1853).
- ¹⁸G. Kresse and J. Furthmüller, *Comput. Mater. Sci.* **6**, 15 (1996).
- ¹⁹P. E. Blöchl, *Phys. Rev. B* **50**, 17953 (1994).
- ²⁰G. Kresse and D. Joubert, *Phys. Rev. B* **59**, 1758 (1999).
- ²¹D. Alfè, *Comput. Phys. Commun.* **118**, 31 (1999).
- ²²S. Nosé, *Mol. Phys.* **52**, 255 (1984); *J. Chem. Phys.* **81**, 511 (1984).
- ²³G. V. Chester and A. Thellung, *Proc. Phys. Soc., London* **77**, 1005 (1961).
- ²⁴M. P. Desjarlais, J. D. Kress, and L. A. Collins, *Phys. Rev. E* **66**, 025401 (2002).
- ²⁵H. J. Monkhorst and J. D. Pack, *Phys. Rev. B* **13**, 5188 (1976).
- ²⁶A. Baldereschi, *Phys. Rev. B* **7**, 5212 (1973).
- ²⁷S. Mazevet, M. Torrent, V. Recoules, and F. Jollet, *High Energy Density Phys.* **6**, 84 (2010).
- ²⁸A. J. Greenfield, J. Wellendorf, and N. Wisser, *Phys. Rev. A* **4**, 1607 (1971).
- ²⁹G. Kresse and J. Hafner, *Phys. Rev. B* **47**, 558 (1993).
- ³⁰The experimental value of σ_0^{expt} at 400 K is obtained by interpolating the results reported by J. F. Freedman and W. D. Robertson, *J. Chem. Phys.* **34**, 769 (1961).
- ³¹E. Evangelisti and F. Isacchini, *Int. J. Heat Mass Transfer* **8**, 1303 (1965).